International Journal of Pharmacy and Biological Sciences-IJPBS™ (2019) 9 (2): 551-560
Online ISSN: 2230-7605, Print ISSN: 2321-3272
Research Article | Biological Sciences | Open Access | MCI Approved
UGC Approved Journal

Extracellular Synthesis of Metal Nanoparticles by *Azospirillum brasilense*: Promising Antimicrobial, Anti-inflammatory, Antiproliferative and Anti-Angiogenic Agents

H. P. Spoorthy[1,2], N. Chandra Mohana[1], B. R. Nuthan[1] and S. Satish[*1]
[1]DOS in Microbiology, University of Mysore, Mysuru-06, Karnataka, India.
[2]Department of Microbiology, JSS College, B. N. Road, Mysuru-25, Karnataka, India.

Received: 17 Jan 2019 / Accepted: 19 Mar 2019 / Published online: 1 Apr 2019
Corresponding Author Email: satish.micro@gmail.com

Abstract
Emergence of antibiotic resistance has been a major concern; the Nano biotechnology has envisioned to meet this prerequisite challenge. In this present work we have evaluated the efficacy of zinc, copper and nickel nanomaterials biosynthesized from *Azospirillum brasilense*. The nanoparticles synthesised extracellularly were characterised using spectroscopic techniques such as UV-visible, FT-IR SEM and XRD. The synthesized nanoparticle was evaluated for antimicrobial against microbial pathogens. Few nanoparticles showed significant antimicrobial and anti-inflammatory activities. All the nanoparticles exhibited good antiproliferative and anti-angiogenic activity.

Keywords
Azospirillum brasilense, Antimicrobial, Anti-inflammatory, antiproliferative, anti-angiogenic.

*****

INTRODUCTION
Nanoparticles have been centre of attraction for researchers for their multifaceted abilities. Synthesis of nanoparticles by biological methods using various microorganisms have attracted a tremendous attention as these are non-toxic, economical and form an alternative to physical and chemical method. Metal microbial interaction has gained interest in the last few years because the synthesis of nanoparticles has been reported from bacteria, yeast, fungi and other biological sources [1-6] with various biopotential. Antibiotics conjugated with nanoparticles would enable better efficacy, delivery and protection against human pathogens as well as treatment various other ailments [7- 9]. From the discovery of antimicrobial drugs in the 1960, several communicable diseases were prevented [10]. The action of antimicrobials varies and it includes the inhibition of the synthesis of DNA or they can even kill the microorganisms by affecting the metabolic pathways [11]. The mechanisms developed by the microorganisms to resist the antimicrobials may be endogenous or exogenous in nature, which includes mutation in the genes or resistance developed by the

decreased permeability of drugs [12, 13]. The development of new metal nanoparticles synthesized by green synthesis and their antimicrobial activity [14]. These particles have a high surface-to-volume ratio and vary from 0.2-100 nm in size [15]. The physico-chemical properties of nanoparticles change from those of their bulk materials. This may be accredited to their high surface to volume ratio [16, 17]. From ancient times silver has been used for the treatment of wounds and inflammation [18]. It has been used since ancient times for the treatment of inflammation which have potent anti-inflammatory [19] and antioxidant activity [20].

In this study we have employed *Azospirillum* spp. which is plant growth-promoting bacteria, apart from symbiotic rhizobia [21-22]. Plant associated nitrogen fixing soil bacteria *Azospirillum brasilense* were shown to reduce the Copper, Nickel and Zinc, resulting in the formation of metal nanoparticles [23]. The nanoparticles were evaluated for the antimicrobial, anti-inflammatory, antiproliferative and anti-angiogenic activity.

MATERIALS AND METHODS

Chemicals required for the biosynthesis of nanoparticles like copper sulfate, nickel chloride, zinc nitrate and Dimethyl sulfoxide were obtained from SDFCL (Mumbai, India). The bacterial strain used for the nanoparticle synthesis, *Azospirillum brasilense* (NCIM-5135) was obtained from NCL, Pune. Culture media and standard antibiotics; muller hinton agar (MHA) potato dextrose agar (PDA), nutrient broth (NB), elliker broth (EB), Luria Bertani broth (LBB), gentamicin and nystatin, were purchased from Hi Media (Mumbai, India). Human pathogenic cultures of Gram-positive bacteria such as *Staphylococcus aureus* (MTCC 7443), *Streptococcus orilies* (MTCC 389), *Streptococcus mitis* (MTCC 2696), *Bacillus cereus* (MTCC 9762) and Gram-negative bacteria such as *Escherichia coli* (MTCC 7410), *Klebsiella pneumonia* (MTCC 7407), *Proteus mirabilis* (MTCC 425), *Pseudomonas aerogenosa* (MTCC 7903), *Salmonella typhimurium* (MTCC 1254), *Shigella flexneri* (MTCC 9543), *Salmonella paratyphi* (MTCC 3220) were procured from Microbial Type Culture Collection (MTCC), Chandigarh, India. Pathogenic fungi such as *Fusarium oxysporum* (MTCC 3656), *Helminthosporium solani* (MTCC 2075) and *Aspergillus niger* (MTCC 478) were procured from DANIDA laboratory, University of Mysore, Mysuru. Human metastatic breast cancer (MDA-MB 231), human chronic myeloid leukemia (K562), human colon carcinoma (Colo-205) and human neuroblastoma (IMR-32) cell lines were procured from the National Center for Cell Sciences in Pune, India. All cells were grown in RPMI-1640 supplemented with 10% heat-inactivated FBS, 100 IU/mL penicillin, 100 mg/mL streptomycin and 2mM glutamine. The cultures were maintained in a humidified atmosphere with 5% CO_2 at 37 °C. Diclofenac sodium was purchased from Sigma-Aldrich (Bengaluru).

Biosynthesis of nanoparticles

Azospirillum brasilense culture was prepared in LB broth maintained for 24 hrs at 37 °C along with shaking 200 rpm. Cell-free supernatant (CFS) of *A. brasilense* for the nanoparticle synthesis was separated by centrifugation at 8000 rpm for 20 min. Heavy metals mediated biosynthesis of nanoparticles was carried out by mixing 90 ml CFS and 10 ml of a 1mM solution of copper sulfate, nickel chloride, and zinc nitrate respectively and incubated at 30 °C for 24 hrs in a dark environment. Biosynthesized nanoparticles were further concentrated by centrifugation at 10,000 rpm for 5 min twice and collected for further characterization.

Optimization of nanoparticle biosynthesis

Media

Influence of the culture media on *A. brasilense* for the biosynthesis of nanoparticles was determined using different culture media such as NB, EB, and LBB. The yield of the biosynthesized nanoparticles was expressed as µg ml^{-1}.

pH

Effect of *pH* influencing the nanoparticles biosynthesis was carried out by varying the pH of the reaction mixture at *pH* 3, 7 and 11 respectively. Optimum *pH* for the biosynthesis of metal nanoparticles determined by the yield which was expressed as µg ml^{-1}.

Temperature

The reaction mixture of the metal salts and the cell-free supernatant of *A. brasilense* was incubated at three different temperatures at 30 °C, 40 °C and 50 °C respectively. A suitable temperature for the biosynthesis of nanoparticles was determined by monitoring the yield.

Characterization of nanoparticles

UV-Visible spectral analysis

Biosynthesized nanoparticles were studied using Agilent, CARY 60 UV-Vis spectrophotometer absorption spectra through a quartz cuvette with 1cm path length. Then the surface Plasmon resonance characterized against a reference sample [24].

Fourier Transform Infra-Red (FT-IR) Spectroscopy

FT-IR analysis determines the functional groups present in biosynthesized nanoparticles. Powdered sample was placed on a 1 mm diameter hole of 0.05 mm thick anti-corrosive steel gasket mounted on a diamond anvil cell of Agilent FT-IR ATR Cary 630. Spectral data was recorded from the range of 7000–350 cm^{-1} with a resolution of 4 cm^{-1} [24].

Scanning Electron Microscopy (SEM) Analysis

Biosynthesised nanoparticleswere washed and diluted in distilled water to reach an absorbance range of 0.40 OD. Image analysis was carried out using a drop of bio-nanoparticles layered on a carbon-coated copper and air dried *in-vacuo*. After drying, the bio-nanoparticles were visualized using HITACHI (S-3400N, Japan) with voltage acceleration of 10 kV.

X-ray diffraction (XRD) Analysis

XRD measurements of biosynthesized nanoparticles were performed on a Rigaku Desktop Miniflex II X-ray powder diffractometer with Cu kα radiation, (λ=1.5406 A°) as the energy source. The obtained peak positions were compared with standard files to identify the crystalline phase [24]. The size of the particles was calculated using Scherer's formula:

$$D = \frac{k\lambda}{\beta \cos\theta}$$

Where D is the crystalline size, λ is the wavelength of X-ray used; K is the shape factor, β is the full line width at the half maximum (FWHM) elevation of the main intensity peak, and θ is the Bragg angle. Philips PAN analytical machine was employed for nanoparticles identification using X-ray diffraction studies with a scanning range of 20˚-130˚ and bond angle of 3˚.

Antibacterial assay

Antibacterial activity of the biosynthesized nanoparticles was evaluated against seven Gram-negative bacteria (*E. coli, Kl. pneumonia*, *Pr. mirabilis*, *Ps. Aerogenosa, Salm. typhimurium*, *Salm. Paratyphi* and *Sh. flexneri*) and four Gram-positive bacteria (*B. cereus, Staph. Aureus, Strep. orilies* and *Strep mitis*) by disc diffusion assay. Sterile discs (6 mm) were amended with 20 µL of two different concentrations (50 and 100 µg $disc^{-1}$) of nanoparticle solution and placed on the MHA plates, whichwere previously seeded with standardized test inoculum. Heavy metal solution and CFS used as assay controls (20 µL $disc^{-1}$), gentamicin (10 µg $disc^{-1}$) as positive control respectively [24].

Antifungal activity

Antifungal activity of biosynthesized nanoparticles was evaluated by percent inhibition of pathogenic fungi using poisoned food technique [26]. Biosynthesized nanoparticles were tested against three plant pathogenic fungi *A. niger, F. oxysporum,* and *H. solani.* Pathogenic fungi were inoculated on to PDA plates previously amended with 50, 100, and 200 µg ml^{-1} concentrations of nanoparticles. The Petri plates containing media devoid of nanoparticle served as assay control, and Nystatin was used as positive control. Petri plates were incubated at 25 ± 2 °C for 7 days, and the colony diameter was measured in mm (Singh and Tirupathi, 1999). Toxicity of the nanoparticles was measured in terms of percentage inhibition of mycelial growth was calculated using the formula,

% Inhibition = C-T/C x 100

C= Average increase in mycelia growth in control plate.

T = Average increase in mycelia growth in treatment plate.

Anti-inflammatory assay

A semi-quantitative indirect hemolytic assay was employed to detect the anti-inflammatory activity of the biosynthesized nanoparticles. Briefly, packed human erythrocytes, egg yolk, and phosphate buffer saline was mixed (1:1:8 V/V), and 1ml of this suspension was incubated with 60 µg enzyme for 10 min at 37 °C. The reaction was stopped by adding 9 ml of cold phosphate buffer saline and centrifuged at 4 °C for 10 min at 800xg. The amount of hemoglobin released in the supernatant was measured at 540 nm [27]. The assay was also carried out in the presence of concentrations of 200 µg/ml of nanoparticles. Lysis of erythrocytes by adding 9 ml of distilled water to the control reaction mixture was taken as 100%. The resulting turbidity was measured at 600 nm, and the percentage inhibition was calculatedas follows, Percentage of inhibition (%) = (OD of Control – OD of Sample / OD of Control) x 100. Diclofenac sodium was used as standard and treated similarly for determination of absorbance.

Antiproliferative activity

The 3-(4,5-di methyl thiazol-2-yl) -2, 5-di phenyl tetrazolium bromide (MTT) assay was used for the investigation of potential effects of biosynthesized nanoparticles on cell viability [28]. A known number of cells (human cancer cell lines, $5.0x10^3$) are transferred into 96 well plates in a volume of 200 µL of culture medium and incubated for 48 hours before the addition of nanoparticles. Cells are then exposed to known concentrations of the biosynthesized nanoparticles to be tested (10 µM expressed as a final concentration) for 24 hours at 37 °C. After exposure to biosynthesized nanoparticles, the culture medium was removed and 20 µl (diluted in culture medium, 5 mg/ml) MTT reagent was added.

After 4 hours of incubation, MTT reagent was removed, and solvent (100 µl) was added to each well, and plates are agitated for 1 min, and absorbance was recorded at 570 nm. Results are expressed by comparing the absorbance of the wells containing nanoparticle treated cells with the absorbance of wells containing 0.1 % solvent alone.

Anti-angiogenic activity

Chorioallantoic membrane assay was performed according to the method [29]. The fertilized eggs were divided into different treatment groups, which included control, the vehicle-treated group and metal nanoparticle treated groups with a minimum of six eggs in each group. The fertilized eggs were incubated for 6 days at 37 °C in a humidified and sterile atmosphere. The window was made on the egg shell to assess the developmental stage of the embryo and was resealed and incubation was continued. On day 8 the windows were opened, and the compound/vehicle was loaded on the Whattman filter paper discs separately, air dried and inverted over the CAM and the windows were closed. The window was resealed and the embryo was allowed to develop further. The windows were opened and observed on day 9 and inspected for changes in the micro vessel density in the area around the paper discs.

RESULTS AND DISCUSSION

Optimization of nanoparticle biosynthesis

Media

Yield of metal nanoparticles was more in Luria-Bertani (LB) media, followed by Nutrient Broth (NB) and Elliker Broth (EB) **(Table 1)**.

pH

The pH range of 3-11 were analysed for effect of pH and yield. The maximum production was achieved at pH 7 in LB media for all the metal NPs **(Table 2)**.

Temperature

The varying temperature of 30ºC, 40ºC and 50ºC was employed to determine the maximum yield. Microorganism produces maximum amount of silver nanoparticles at 40 ºC in LB media **(Table 3)**. This result indicated that elevated temperature influenced the synthesis of nanoparticles.

UV-Visible spectral analysis

The preliminary confirmation was observed by color change followed by UV-Visible spectral analysis. The samples were monitored for every minute and maximum synthesis was achieved at 15 minutes and the UV absorbance was recorded. CuNPs formation was confirmed by the absorption at 575 nm, NiNPs at 370 nm, and ZnNPs showed maximum peak absorption at 410 nm (**Figure 1**).

Fourier Transform Infra-Red (FT-IR) Spectroscopy

FT-IR Spectral characterization of metal nanoparticles revealed in **Figure 2**. The 3300–2800 cm^{-1} spectral region is the fatty acid region, 1700-1500 cm^{-1} contains the carboxylic acid, 1500-1200 cm^{-1} is a mixed region of fatty acid bending vibrations, 1200-900 cm^{-1} contains absorption bands of the carbonyl group of polysaccharides in microbial cell walls and 450 to 550 cm^{-1} contains the C=O bending frequency is the fingerprint region that contains weak but very unique absorbance that are characteristic to specific microorganism.

Scanning Electron Microscopy (SEM) Analysis

The surface morphological characteristics of *Azospirillum brasilense* CuNPs, NiNPs and ZnNPs was analyzed using Scanning Electron Microscopy. The analysis revealed the polydispersity of metal nanoparticles.

X-ray diffraction (XRD) Analysis

The XRD patterns of metal nanoparticles using supernatant *Azospirillum brasilense* culture as represents the diffraction peak at 2θ values assigned to (111), (200), (220) and (311) of lattice plane of face centered cubic (FCC) of nanoparticles. The XRD pattern clearly showed that the synthesized metal nanoparticles formed were composed of pure crystalline and formed by the reduction of metal ions.

Antibacterial assay

The antibacterial activity of Cu, Ni and Zn NPs was investigated against gram negative and gram positive pathogens using well-diffusion method. The mean of three replicates of the diameter of inhibition zones (in millimeters) were recorded and represented in **Table 4**. All the concentrations, biosynthesized Ni and Zn NPs inhibited bacterial growth. The maximum zone of inhibition was observed in CuNPs followed by NiNPs and ZnNPs. CuNPs minimum zone was recorded in *Sh. Flexneri.* NiNPs had minimum against *Pr. Mirabilis*. Similarly, ZnNPs were able to inhibit bacterial growth and a maximum zone of inhibition was observed against *Staph. Aureus* and a minimum zone of inhibition for *Sh. flexneri*.

Antifungal activity

Biosynthesized nanoparticles showed varying degree of percentage inhibition against concentration of 25, 50, 100 and 200µg/ml against *Aspergillus niger, Fusarium oxysporum* and *Helminthosporium solani* **(Table 5)**. The maximum activity was exhibited at concentration of 200 µg/ml against tested pathogens for all NP's there was no significant variation with respect to inhibition.

Anti-inflammatory assay

Increased PLA_2 activity is responsible for the inflammation in many diseases. The ZnNPs had significant IC50 values when compared to the other nanoparticles **(Table 6)**. No significant inhibition was observed with copper and nickel nanoparticles.

Antiproliferative activity

The antiproliferative actions of nanoparticles were tested against four different cell lines. The activity was evaluated by measuring the levels of surviving cells after incubation for 24h with the test samples, using the MTT colorimetric assay, based on the ability of metabolically active cells to convert the pale yellow MTT to a blue formazan product which is quantifiable spectrophotometrically. Percentage of cell survival for tested samples against MDA-MB 231, K562, Colo-205 and IMR-32 cells is tabulated in **Table 7**. The results were expressed as percentage of cell proliferation compared with cells in control (cells treated with vehicle, 0.1% DMSO) **(Figure 3)**.

Anti-angiogenic activity

The investigation of anti-angiogenic activity of *Azospirillum brasilense* mediated nanoparticles such as CuNPs, NiNPs, and ZnNPs in chorioallantoic membrane (CAM) assay showed significant reduction of proliferation of capillaries around the zone of application of the discs loaded with the nanoparticles as compared to the control site where only the vehicle, 0.1% polyethylene glycol (PEG) were applied. These results indicate that the metal nanoparticles are potent anti-angiogenic molecules in vivo. The angio-inhibitory activity of the metal nanoparticles is as shown in the **Figure 4** exhibiting significant positive results in the CAM assay model of developing embryos.

The investigation of anti-angiogenic activity of *Azospirillum brasilense* mediated nanoparticles such as CuNPs, NiNPs, and ZnNPs in chorioallantoic membrane (CAM) assay showed significant activity. These results indicate that the above metal nanoparticles exhibiting significant positive results in this model of developing embryos. The CAM assay has been proved as a reliable in vivo model to study angiogenesis and many inhibitors and stimulators of angiogenesis have been examined by this common method.

Table 1: Yield of metal nanoparticles (µg/ml) by *Azospirillum brasilense* in different media

Nanoparticles	LB	NB	EB
	Yield in µg/ml		
Copper	73.5	72.1	70.2
Nickel	65.2	64.2	62.3
Zinc	56.3	53.0	51.1

Table 2: The effect of pH in LB media on the production of nanoparticles

Nanoparticles	pH- 3	pH- 7	pH-11
	Yield in µg/ml		
Copper	72.3	73.0	70.0
Nickel	64.1	65.0	62.3
Zinc	53.2	56.3	51.5

Table 3: Effect of temperature on the production of nanoparticles

Nanoparticles	30ºC	40ºC	50ºC
	Yield in µg/ml		
Copper	71.3	73.4	72.5
Nickel	61.1	65.0	62.3
Zinc	51.5	56.0	53.7

Table 4: Antibacterial activity of *A. Brasilense* nanoparticles at different concentrations against pathogenic bacteria

Test sample	Conc. µg/disc	Zone of Inhibition in mm										
		B. cereus	***Staph. aureus***	***Strep. mitis***	***Strep. oralis***	***E. coli***	***Kl. pneumonia***	***Pr. mirabilis***	***Ps. aerogenosa***	***Salm. paratyphi***	***Salm. typhimurium***	***Sh. flexneri***
Copper	**Control**	11.3 ± 0.58 ^{gh}	10.0 ± 1.00 ^{hi}	9.3 ± 0.58^{ghi}	7.3 ± 0.58 ^{ij}	10.0 ± 1.00^{ij}	7.3 ± 0.58 ^{j}	8.0 ± 0.00^{jk}	11.7 ± 0.58 ^{hi}	6.7 ± 0.58 ^{k}	9.0 ± 0.00 ^{ij}	8.3 ± 0.58 ^{hi}
	50	15.3 ± 0.58 ^{ef}	16.7 ± 0.58 ^{cd}	13.7 ± 0.58 ^{de}	13.0 ± 1.00 ^{ef}	18.3 ± 0.58 ^{e}	12.3 ± 0.58 ^{hi}	17.7 ± 0.58 ^{c}	19.0 ± 1.00 ^{de}	11.7 ± 0.58 ^{h}	12.0 ± 1.00^{ef}	10.3 ± 0.58^{gh}
	100	24.0 ± 1.00 ^{b}	22.0 ± 1.00 ^{ab}	22.0 ± 1.00 ^{a}	21.7 ± 0.58 ^{a}	23.7 ± 0.58 ^{ab}	21.7 ± 0.58 ^{b}	25.7 ± 0.58 ^{a}	31.0 ± 1.00 ^{a}	21.7 ± 0.58 ^{a}	19.0 ± 0.00 ^{b}	19.3 ± 0.58 ^{ab}
Nickel	**Control**	9.3 ± 0.58 ^{hi}	8.3 ± 0.58 ^{i}	10.3 ± 0.58 ^{fgh}	8.7 ± 0.58 ^{hi}	13.0 ± 1.00^{gh}	11.3 ± 0.58 ^{i}	8.3 ± 0.58^{ijk}	10.7 ± 0.58 ^{i}	11.3 ± 0.58 ^{h}	11.3 ± 0.58 ^{fgh}	8.7 ± 0.58 ^{hi}
	50	16.7 ± 1.15 ^{e}	18.0 ± 1.00 ^{c}	15.0 ± 1.00 ^{cd}	16.0 ± 0.00 ^{bcd}	20.0 ± 1.00 ^{cde}	19.0 ± 1.00 ^{c}	14.0 ± 0.00^{efg}	18.7 ± 0.58 ^{de}	17.0 ± 0.00 ^{def}	19.0 ± 1.00 ^{b}	16.3 ± 1.53 ^{cd}
	100	20.0 ± 1.00 ^{d}	17.0 ± 1.00 ^{cd}	19.0 ± 1.00 ^{b}	20.0 ± 1.00 ^{a}	26.0 ± 1.00 ^{a}	23.7 ± 0.58 ^{a}	16.7 ± 0.58 ^{cd}	27.3 ± 1.15 ^{b}	18.7 ± 1.53 ^{bcd}	23.3 ± 0.58 ^{a}	17.7 ± 0.58 ^{bc}
Zinc	**Control**	8.7 ± 0.58 ^{i}	16.3 ± 0.58 ^{cd}	9.0 ± 0.00 ^{hi}	10.7 ± 0.58 ^{gh}	12.0 ± 1.00 ^{hi}	7.3 ± 0.58 ^{j}	8.7 ± 0.58^{hijk}	14.0 ± 1.00 ^{gh}	10.0 ± 1.00 ^{hi}	9.3 ± 0.58 ^{hi}	7.3 ± 0.58 ^{i}
	50	13.0 ± 0.00 ^{fg}	23.0 ± 1.00 ^{a}	14.7 ± 1.53 ^{cd}	14.3 ± 0.58 ^{de}	20.0 ± 1.00 ^{cde}	13.0 ± 1.00 ^{ghi}	14.7 ± 0.58 ^{def}	20.0 ± 1.00 ^{cd}	13.3 ± 0.58 ^{g}	15.3 ± 0.58 ^{cd}	12.7 ± 1.15 ^{ef}
	100	15.3 ± 0.58 ^{ef}	23.7 ± 0.58 ^{a}	15.7 ± 0.58 ^{cd}	17.7 ± 0.58 ^{b}	21.7 ± 0.58 ^{bcd}	13.3 ± 0.58^{gh}	15.7 ± 0.58 ^{cde}	21.0 ± 1.00 ^{cd}	16.3 ± 0.58^{ef}	15.7 ± 0.58 ^{cd}	13.0 ± 1.00^{ef}
Gentamicin	**10**	21.0 ± 1.00 ^{cd}	23.0 ± 1.00 ^{a}	19.3 ± 0.58 ^{b}	21.3 ± 0.58 ^{a}	22.7 ± 0.58 ^{b}	18.3 ± 0.58 ^{cd}	21.3 ± 1.53 ^{b}	22.3 ± 1.53 ^{c}	19.3 ± 0.58^{bc}	20.3 ± 1.53 ^{b}	20.0 ± 1.00 ^{a}
Culture filtrate	**25 µL**	- NIL -	- NIL -	- NIL -	- NIL -	- NIL -	- NIL -	- NIL -	- NIL -	- NIL -	- NIL -	- NIL -

Values expressed are means of triplicates ± standard deviation of the mean (SDM; significant $p < 0.001$) by one-way ANOVA, followed by the same superscript letter(s) within columns are significantly different at $p < 0.05$ by Tukey's post hoc test.

Table 5: Antifungal activity of *A. Brasilense* nanoparticles at different concentrations against pathogenic fungi

Test Sample	Conc. (µg/ml)	% Inhibition		
		Aspergillus niger	*Fusariumoxy sporum*	*Helminthosporium solani*
Copper	50	NIL	NIL	NIL
	100	62.81 ± 0.56 ^{jk}	68.41 ± 0.48 ^{c}	61.97 ± 0.38 ^{k}
	200	65.87 ± 0.61 ^{hi}	69.77 ± 0.65 ^{c}	63.78 ± 0.15 ^{j}
Nickel	50	NIL	NIL	NIL
	100	61.77 ± 0.57 ^{k}	63.37 ± 0.26 ^{ef}	64.10 ± 0.21 ^{j}
	200	63.61 ± 0.26^{ijk}	64.68 ± 0.35 ^{de}	65.64 ± 0.33 ^{hi}
Zinc	50	NIL	NIL	NIL
	100	64.23 ± 0.35 ^{ij}	63.44 ± 0.47 ^{ef}	64.44 ± 0.37 ^{ij}
	200	66.81 ± 0.34 ^{h}	65.67 ± 0.41 ^{d}	66.63 ± 0.46 ^{h}
Nystatin	50	81.76 ± 0.36 ^{c}	68.32 ± 0.41 ^{c}	83.17 ± 0.63 ^{c}
	100	84.89 ± 0.49 ^{b}	73.97 ± 0.38 ^{b}	86.79 ± 0.46 ^{b}
	200	88.86 ± 0.69 ^{a}	80.07 ± 0.33 ^{a}	88.90 ± 0.31 ^{a}

Values expressed are means of triplicates ± standard deviation of the mean (SDM; significant $p < 0.001$) by one-way ANOVA, followed by the same superscript letter(s) within columns are significantly different at $p < 0.05$ by Tukey's post hoc test.

Table 6: IC_{50} value of PLA_2 Inhibition by different metal nanoparticles synthesised by *A. brasilense*

Test sample	*Azospirillum brasilense*
	IC_{50} µg/ml
Copper	52.13±1.65
Nickel	50.40±1.10
Zinc	30.11±1.00
Diclofenac sodium	12.80±1.38

Table 7: Antiproliferative activity (in %) of metal NPs determined by MTT assay

Test sample	Cell lines	% cell survival
Copper	MDA-MB 231	66.00±0.20
	K562	61.05±0.24
	Colo-205	68.52±0.22
	IMR-32	64.30±0.10
Nickel	MDA-MB 231	62.50±0.20
	K562	59.50±0.24
	Colo-205	63.22±0.10
	IMR-32	59.15±0.21
Zinc	MDA-MB 231	60.20±0.34
	K562	59.10±0.40
	Colo-205	61.52±0.20
	IMR-32	57.30±0.10
DMSO (Control)	MDA-MB 231	99.90±0.02
	K562	99.90±0.02
	Colo-205	99.90±0.02
	IMR-32	99.90±0.02

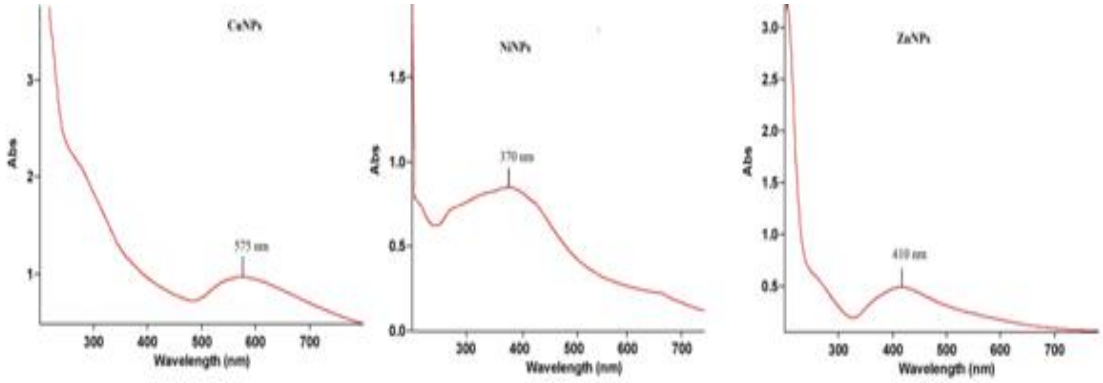

Figure 1: UV absorbance peaks of synthesized nanoparticles

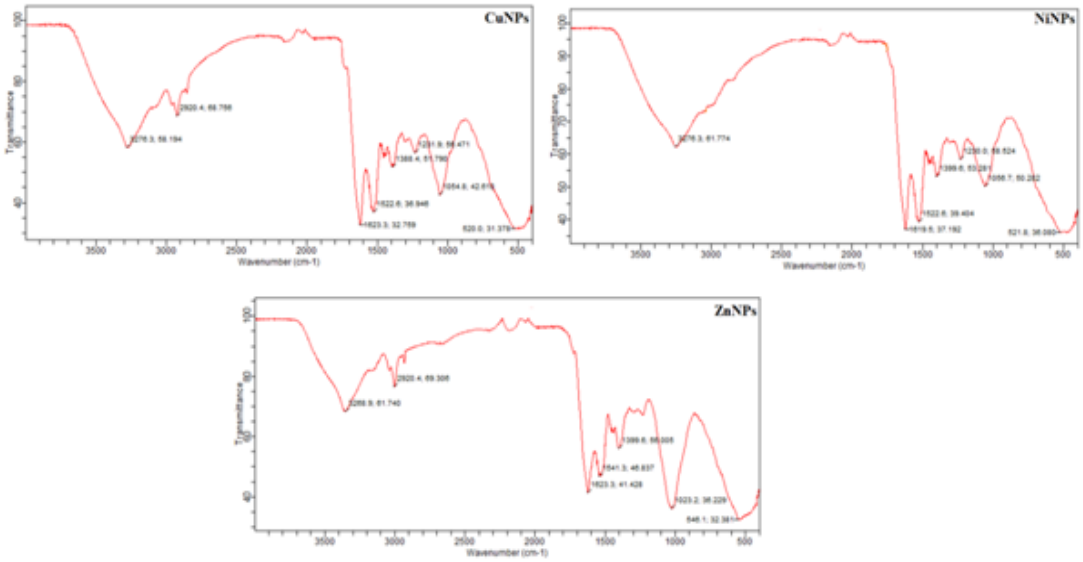

Figure 2: FT-IR Spectral peaks of biosynthesized metal nanoparticles

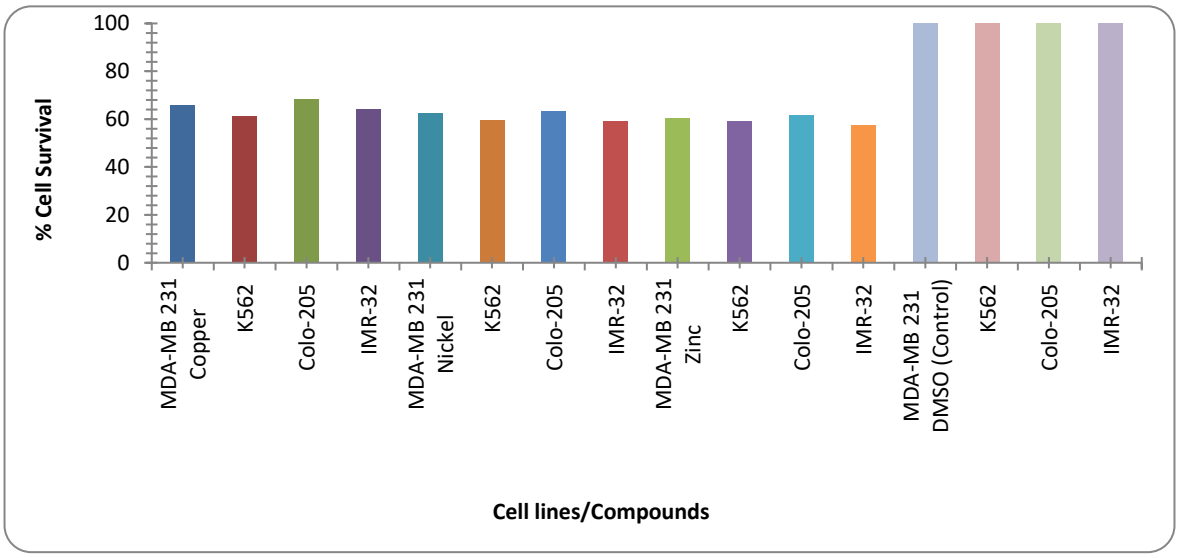

Figure 3: Antiproliferative activity metal nanoparticles

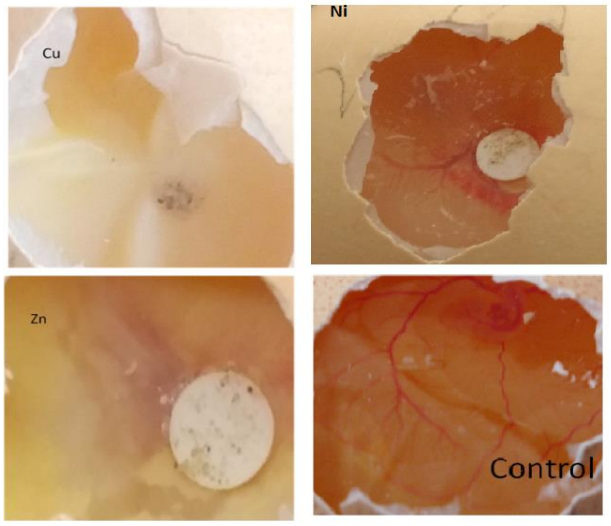

Figure 4: Suppression of angiogenesis by metal nanoparticles in CAM assay model

CONCLUSION

Metal nanoparticles were successfully synthesized using microorganisms. Antimicrobial property reveals that CuNPs and ZnNPs showed good activity and also ZnNPs exhibited good anti-inflammatory property. Copper and Nickel nanoparticles exhibited significant antiproliferation against cell lines and all the NPs showed significant positive results in this model of developing embryos. In the upcoming years efforts, have been made in synthesis of NPs from microorganism in large scale and their commercial application in biomedical fields such as health and medicine.

ACKNOWLEDGEMENTS

The authors are thankful to the DOS in Microbiology, Manasagangotri, University of Mysore and JSS College, Mysore, India for providing facility and infrastructure.

REFERENCES

[1] Shankar SS., Ahmad A., Sastry M. Geranium leaf assisted biosynthesis of silver nanoparticles. Biotech. Prog. 19(6):1627-1631, (2003).

[2] Ankamwar B., Damle C., Ahmad A., Sastry M. Biosynthesis of gold and silver nanoparticles using emblica officinalis fruit extract. J. Nanosci. Nanotechnol. 5(10):1665-1671, (2005).

[3] Bhainsa KC., D'Souza SF. Extracellular biosynthesis of silver nanoparticles using the fungus aspergillus fumigates. Coll. Surf. B Biointer. 47(2):160-164, (2006).

[4] Lengke MF., Fleet ME., Gordon S. Biosynthesis of silver particles filamentous cyanobacteria from a silver(I) nitrate complex. Langmuir. 23(5):2694-2699, (2007).

[5] Naik RR., Stringer SJ., Agarwal G., Jones SE., Stone MO. Biomimetic synthesis and patterning of silver nanoparticles. Nature Mater. 1(3):169-172, (2002).

[6] Duran N., Marcato PD., Alves OL., De Souza GIH., Esposito E. Mechanistic aspects of biosynthesis of silver nanoparticles by several fusarium oxysporum strains. J. Nanobiotech. 3(1):1-7, (2005).

[7] Joerger R., Klaus T., Granquist CG. Biologically produced silver carbon composite materials for optically functional thin film coatings. Adv. Mater. 12(6):407-409, (2000).

[8] Mukherjee P., Ahmad A., Mandal DS., Senapati S., Sainkar R., Khan MI., Parishcha R., Ajaykumar PV. Silver nanoparticles and their immobilization in the mycelial matrix: A novel biological approach to nanoparticle synthesis. Nano Lett. 1(10):515-519, (2001).

[9] Von Nussbaum F., Brands M., Hinzen B., Weigand S., Habich D. Antibacterial natural products in medicinal Chemistry-Exodus or revival. Angew. Chem. Int. Ed. 45(31):5072-5129, (2006).

[10] Oates A., Hu Y., Bax R., Page C. The future challenges facing the development of new antimicrobial drugs. Nat. Rev. Drug Discov. 1(11):895-910, (2002).

[11] Awad HM., Kamal YES., Aziz R., Sarmidi MR., El-Enshasy HA. Antibiotics as microbial secondary metabolites: Production and application. J. Teknol. 59(1):101-111, (2012).

[12] Chmieder R., Edwards R. Insights into antibiotic resistance through metagenomic approaches. Future Microbiol. 7(1):73-89, (2012).

[13] Crumplin GC., Odell M. Development of resistance to ofloxacin. Drugs 34(2):1-8, (1987).

[14] Akhtar M., Swamy MK, Umar A, Sahli A, Abdullah A. Biosynthesis and characterization of silver nanoparticles from methanol leaf extract of cassia didymobotyra and assessment of their antioxidant

and antibacterial activities. J. Nanosci. Nanotechnol. 15(12):9818-9823, (2015).

[15] Ravishankar Rai V., Jamuna Bai A. Nanoparticles and their potential application as antimicrobials. Curr. Res. Technol. Adv. 16(2):197-209, (2011).

[16] Hajipour JM., Fromm KM., Ashkarran AA., de Aberasturi DJ., de Larramendi I.R., Rojo T., Serpooshan V., Parak W.J., Mahmoudi M. Antibacterial properties of nanoparticles. Trend Biotechnol. 30(10):499-511, (2012).

[17] Whitesides G.M. Nanoscience, nanotechnology and chemistry. Small. 1(2):172-179, (2005).

[18] Ricciotti E., Fitzgerald GA. Prostaglandins and inflammation. Arterioscler Thromb. Vasc. Biol. 31(5):986-1000, (2011).

[19] Wong KK., Cheung SO., Huang L., Niu J., Tao C. Further evidence of the anti-inflammatory effects of silver nanoparticles. Chem. Med. Chem. 4(7):1129-1135, (2009).

[20] Jeyaraj M., Sathishkumar G., Sivanandhan G., MubarakAli D., Rajesh M. Biogenic silver nanoparticles for cancer treatment: An experimental report. Coll. Surf. B Biointer. 106(1):86-92, (2013).

[21] Bashan Y., de-Bashan LE. How the plant growth-promoting bacteria Azospirillum promotes plant growth abcritical assessment. Adv. Agron. 108(10):77-136, (2010).

[22] Tugarova AV., Vetchinkina EP., Loshchinina EA., Burov AM., Nikitina VE., Kamnev AA. Reduction of selenite by *azospirillum brasilense* with the formation of selenium nanoparticles, Microbial. Eco. 68(3):95-503, (2014).

[23] Kupryashina MA., Vetchinkina EP., Burov AM., Ponomareva EG., Nikitina VE. Biosynthesis of gold nanoparticles by *azospirillum brasilense*. Microbio. 82(3):833-840, (2013).

[24] Sandeep S., Santhosh, AS., Swamy NK., Suresh GS, Melo JS., Mallu P. Biosynthesis of silver nanoparticles using Convolvulus pluricaulis leaf extract and assessment of their catalytic, electrocatalytic and phenol remediation properties. Adv. Mater. Lett. 7(12):383-389, (2016).

[25] Pascal JD., Stanich K., Girard B., Mazza G. Antimicrobial activity of individual and mixed fractions of dill, cilantro, coriander and eucalyptus essential oils. Inter. J. Food Microbio. 74(1):101-109, (2002).

[26] Khandelwal N., Singh A., Jain D., Upadhyay MK., Verma H.N. Green synthesis of silver nanoparticles using Argemone Mexicana leaf extract and evaluation of their antimicrobial activities. Digest Journal of Nanomaterials and Biostructures, 5(2):483-489, (2010).

[27] Lowry OH., Rosenbrough NJ., Farr AL., Randall RJ. Protein measurement with the Folin phenol reagent. J. Biol. Chem. 193(1):265-275, (1951).

[28] Mosmann T. Rapid colorimetric assay for cellular growth and survival: application to proliferation and cytotoxicity assays. J. Immunol. Methods, 65(1-2):55-63, (1983).

[29] Nowak-Sliwinska P, Segura TML. The chicken chorioallantoic membrane model in biology, medicine and bioengineering. Angiogenesis, 17(4):779-804, (2014).